Chinese Chemical Letters 37 (2026) 111615

Contents lists available at ScienceDirect

Chinese Chemical Letters

journal homepage: www.elsevier.com/locate/cclet

Photo-induced stereoselective 2-deoxyglycoside synthesis from glycals with carboxylic acids and alcohols

Xianrong Zeng[a,b,1], Hui-Ying Shi[c,1], Huiqian Huang[d,*], Zhaobin Wang[b,e,*]

[a] Department of Chemistry, Zhejiang University, Hangzhou 310058, China
[b] Key Laboratory of Precise Synthesis of Functional Molecules of Zhejiang Province, Department of Chemistry, School of Science and Research Center for Industries of the Future, Westlake University, Hangzhou 310030, China
[c] NHC and CAMS Key Laboratory of Medical Neurobiology, MOE Frontier Science Center for Brain Science and Brain-machine Integration, School of Brain Science and Brain Medicine, Zhejiang University, Hangzhou 310058, China
[d] Basic and Translational Research Center, the Second Affiliated Hospital, Zhejiang University School of Medicine, Hangzhou 310058, China
[e] Institute of Natural Sciences, Westlake Institute for Advanced Study, Hangzhou 310024, China

ARTICLE INFO

Article history:
Received 16 April 2025
Revised 27 June 2025
Accepted 19 July 2025
Available online 21 July 2025

Keywords:
2-Deoxyglycoside
O-Glycosylation
Carboxylic acids
Alcohols
Glycals

ABSTRACT

Synthesizing 2-deoxyglycosides, prevalent motifs in bioactive molecules, presents significant challenges in stereocontrol and functional group tolerance. We report a metal-free, photo-induced *O*-glycosylation of glycals using acridinium salts under visible light. This method effectively couples diverse glycals with both carboxylic acids and alcohols, providing facile access to α-2-deoxyglycosides under mild conditions with broad substrate scope and functional group compatibility. The protocol exhibits high α-stereoselectivity with carboxylic acids and moderate α-selectivity with alcohols, enabling late-stage functionalization of complex molecules, including amino acids, peptides, and drugs. Mechanistic experiments implicate the possible involvement of radical intermediates, potentially operating via a chain reaction. Notably, 2-deoxyglycosylation of NSAIDs using this method enhanced their neuroprotective properties *in vitro*. This photo-induced strategy offers a practical and versatile platform for accessing complex 2-deoxyglycans relevant to medicinal chemistry and chemical biology.

© 2026 Published by Elsevier B.V. on behalf of Chinese Chemical Society and Institute of Materia Medica, Chinese Academy of Medical Sciences.

Carbohydrates, fundamental biomolecules participating in nearly every aspect of life, mediate critical biological processes through their roles in glycoproteins, glycolipids, and polysaccharides, influencing cellular recognition, signaling, immunity, and pathogenesis [1–9]. Within this diverse class, 2-deoxysugars are prominent structural motifs in numerous bioactive natural products, including clinically vital antibiotics and anticancer agents (Fig. 1a) [10–13]. The absence of the C2–hydroxyl group, however, presents unique and significant challenges for their chemical synthesis [14–20]. Traditional glycosylation methods often struggle with controlling the stereochemical outcome at the anomeric center without a participating group at C2, and the inherent reactivity of 2-deoxy donors can lead to undesired side reactions or necessitate harsh conditions incompatible with sensitive substrates [14,20].

Recent advances have witnessed a paradigm shift toward the use of glycals as glycosyl donors. Glycals, by virtue of their electron-rich double bond, offer a distinct advantage by facilitating glycosylation under conditions that minimize side reactions [14,20]. Conventional approaches using these donors have predominantly relied on acid- or metal-mediated activation (Fig. 1b). While powerful, these ionic methods can face issues regarding functional group tolerance and stereocontrol. Organocatalytic alternatives, such as those utilizing electron-deficient pyridinium salts or thioureas, have emerged, offering pathways to 2-deoxyglycosides with notable stereoselectivity, yet often remain rooted in ionic mechanisms or face limitations in substrate scope. Despite these advances, the exploration of fundamentally different activation modes is still in high demand.

Photoredox reaction presents a compelling alternative, enabling the generation of radical intermediates under exceptionally mild conditions and inspiring novel glycosylation approaches [21–27]. Radical-based glycosylations, in particular, offer potential advantages including unique selectivity profiles and compatibility with unprotected substrates [28–34]. Elegant work by Huang and coworkers demonstrated the feasibility of photochemical glycal ac-

* Corresponding authors.
E-mail addresses: hhq0301@zju.edu.cn (H. Huang), wangzhaobin@westlake.edu.cn (Z. Wang).
[1] These authors contributed equally to this work.

https://doi.org/10.1016/j.cclet.2025.111615
1001-8417/© 2026 Published by Elsevier B.V. on behalf of Chinese Chemical Society and Institute of Materia Medica, Chinese Academy of Medical Sciences.

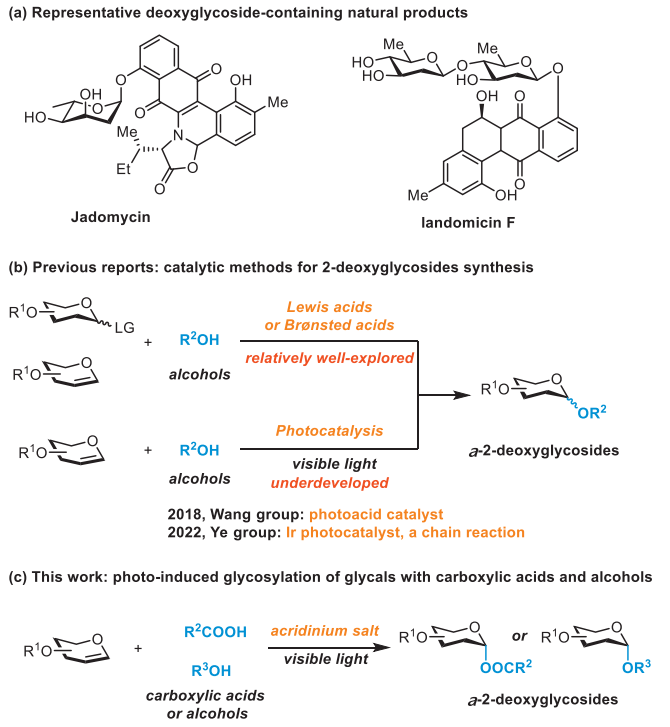


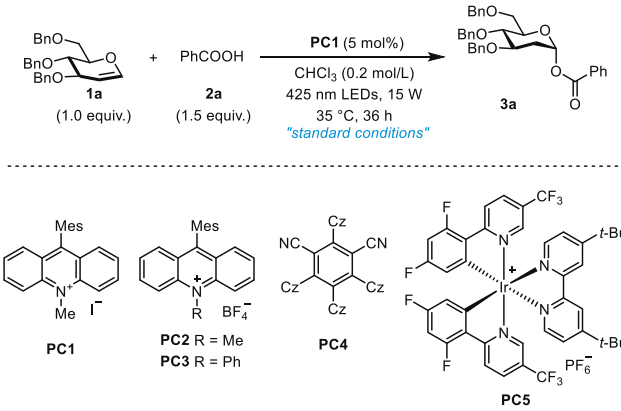
Fig. 1. The importance of 2-deoxyglycosides and their photo-induced synthesis *via* glycals.

tivation for acetal synthesis [35–38], while subsequent contributions from the Wang [39] and Ye [40] groups showcased the power of acridinium photoacids and visible-light promotion, respectively, for the stereocontrolled glycosylation of glycals with alcohols *via* proposed radical cation intermediates. Concurrently, the *O*-glycosylation of carboxylic acids remains a crucial transformation, given the prevalence of acyl glycosides in nature and pharmaceuticals, where glycosylation often enhances solubility and targeting [30,41–45]. Despite progress in radical-based methods using other donors, the direct photo-induced *O*-glycosylation of glycals specifically with carboxylic acids represents an underexplored area.

Herein, we describe a photo-induced, metal-free *O*-glycosylation methodology utilizing catalytic amounts of acridinium salts. This approach harnesses visible light to efficiently couple glycals with both carboxylic acid and alcohol nucleophiles, providing facile access to a diverse range of 2-deoxyglycosides. The transformation proceeds under mild conditions, obviates the need for substrate pre-activation, exhibits excellent stereoselectivity, and demonstrates applicability in the late-stage functionalization of bioactive compounds. By integrating concepts from radical chemistry and photoredox catalysis, this work offers a versatile and practical expansion of the synthetic toolbox for carbohydrate chemistry.

Our investigation commenced with the optimization of the photo-induced *O*-glycosylation using readily available tri-*O*-benzyl-D-glucal (**1a**) and benzoic acid (**2a**) as model substrates (Table 1). A systematic evaluation of reaction parameters revealed that employing 5 mol% of the acridinium salt [22,46] **PC1** in chloroform under 425 nm blue LED irradiation provided the desired α–2-deoxyglycoside **3a** in good yield (75%) and with high diastereoselectivity (19:1 α/β ratio) (Table 1, entry 1). Control experiments confirmed the necessity of both the photosensitizer **PC1** and light irradiation for the reaction to proceed (entries 2 and 3). The photosensitizer loading could be reduced to 2 mol% (**PC1**) with only a minor decrease in efficiency (entry 4). While alternative acridinium salts also facilitated the transformation (entries 5 and 6), common organic photosensitizers like 4CzIPN (**PC4**) or iridium-based photo-

Table 1
Effect of reaction parameters for the 2-deoxyglycosylation of benzoic acid.



Entry	Variations from "*standard conditions*"	Yield (%)[a]	α/β[a]
1	No change	75	19:1
2	Without **PC1**	< 2	–
3	Without light	< 2	–
4	2 mol% **PC1**, instead of 5 mol%	73	12:1
5	**PC2**, instead of **PC1**	54	5:1
6	**PC3**, instead of **PC1**	22	4:1
7	**PC4** or **PC5**, instead of **PC1**	–	–
8	1.2 equiv. **2a**, instead of 1.5 equiv.	65	11:1
9	1.5 equiv. **1a** and 1.0 equiv. **2a**	73	> 20:1
10	DCM, instead of $CHCl_3$	58	> 20:1
11	DCE, instead of $CHCl_3$	60	> 20:1
12	THF, or DMF, instead of $CHCl_3$	< 2	–
13	24 h, instead of 36 h	70	9:1
14	25 °C, instead of 35 °C	61	19:1
15	1.0 mL air was added	48	13:1
16	1.0 equiv. water was added	< 2	–

[a] The yields and ratios were determined *via* ^{1}H NMR analysis with dibromomethane as the internal standard.

sensitizer proved ineffective (entry 7). Variations in stoichiometry showed that using either 1.2 equiv. of benzoic acid (**2a**) or employing **2a** as the limiting reagent maintained reaction efficiency, albeit with slightly lower yields (entries 8 and 9). Solvent screening indicated that chlorinated solvents such as dichloromethane (DCM) and 1,2-dichloroethane (DCE) were also suitable, affording **3a** in good yields (entries 10 and 11), whereas coordinating solvents like tetrahydrofuran (THF) and dimethylformamide (DMF) significantly hampered the reaction (entry 12). The reaction demonstrated robustness with respect to time and temperature, providing comparable results when the reaction time was shortened to 24 h or conducted at ambient temperature (25 °C) (entries 13 and 14). Sensitivity to atmospheric oxygen was observed, as intentional air injection led to a diminished yield (entry 15). Furthermore, the presence of water proved detrimental, completely inhibiting product formation (entry 16), highlighting the need for anhydrous conditions.

With the optimized conditions established (Table 1, entry 1), we next explored the substrate scope with respect to both the glycal donors and carboxylic acid acceptors (Fig. 2). The protocol demonstrated good generality for various glycal derivatives; donors derived from D-glucal, D-galactal, L-rhamnal, and L-fucal, and D-Xylal all participated effectively, furnishing the corresponding 2-deoxyglycosylation products (**3a**–**3h**) in moderate to good yields and with high stereoselectivity. Similarly, a broad range of carboxylic acids proved compatible. Both aliphatic and aromatic carboxylic acids, encompassing varied steric profiles from phenethyl to cyclohexyl groups, reacted smoothly to yield the desired 2-deoxyglycosides (**4a**–**4q**). Significantly, the mild reaction conditions allowed for excellent functional group tolerance. Substrates bear-

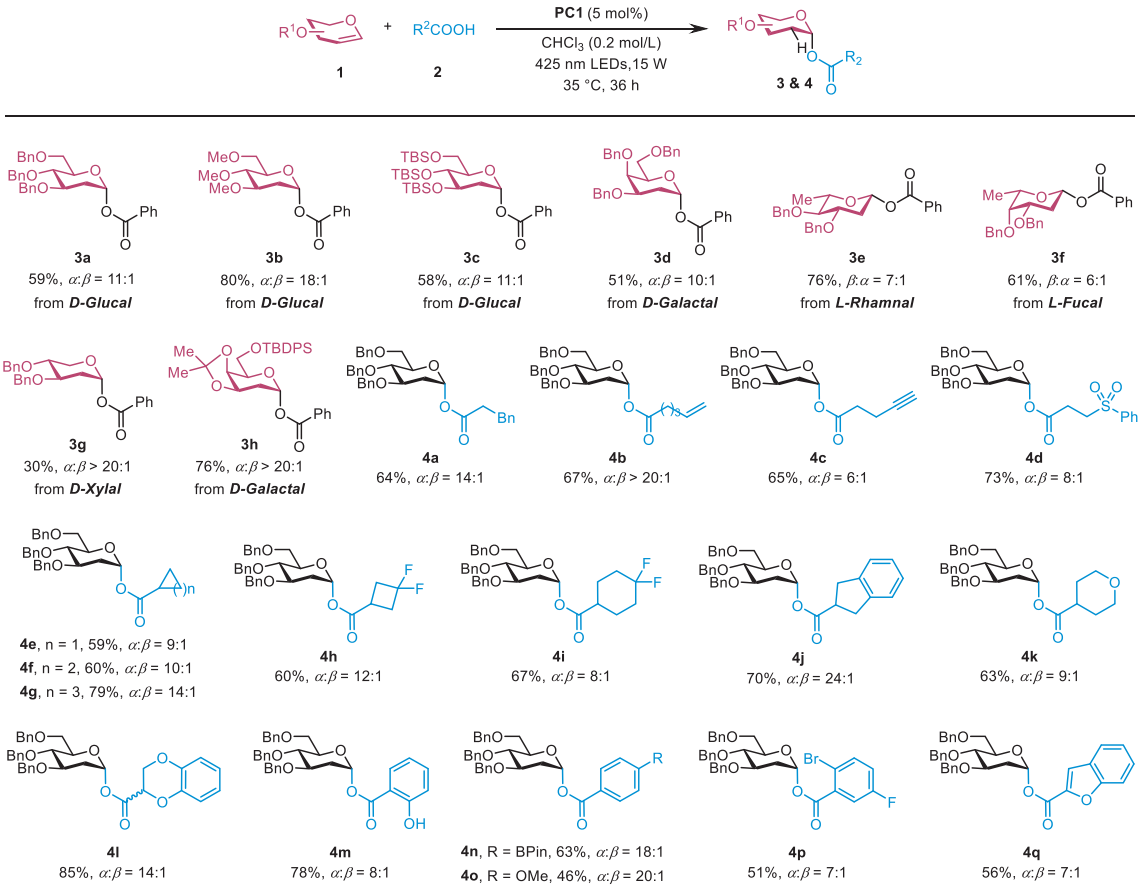


Fig. 2. The scope of glycals and carboxylic acids.

ing terminal olefins (**4b**), terminal alkynes (**4c**), sulfones (**4d**), alkyl fluorides (**4h**), alkyl ethers (**4k**), phenols (**4m**), aryl boronates (**4n**), aryl bromides (**4p**), and benzofurans (**4q**) were all well-tolerated. Increasing steric bulk of the carboxylic acid generally enhances α-selectivity in secondary aliphatic acids (**4e**–**4g**). However, substitution of cyclohexyl with a *gem*–difluoromethylene group in **4i** slightly diminishes selectivity ($\alpha/\beta = 8{:}1$), likely due to the electron-withdrawing nature of the CF_2 unit. The method also exhibited noteworthy chemoselectivity. When salicylic acid was employed, glycosylation occurred preferentially at the carboxylic acid over the phenol group, yielding **4m** as the major product.

The late-stage functionalization of complex molecular scaffolds through glycosylation represents a powerful strategy in modern drug discovery and chemical biology, enabling the diversification of lead compounds and the modulation of pharmacokinetic properties. To demonstrate the utility of our photo-induced *O*-glycosylation protocol in this challenging context, we investigated its application to the modification of amino acid derivatives, bioactive natural products, and approved drugs using glycals as 2-deoxyglycosyl donors. As illustrated in Fig. 3, the reaction proceeded effectively under the optimized conditions, furnishing the desired 2-deoxyglycosylated products (**4r**–**4ak**) in moderate to good yields and exhibiting consistently good α-stereoselectivity. Notably, the methodology proved amenable to the glycosylation of amino acid and dipeptide substrates, showcasing its potential for constructing glycopeptide mimetics, analogous to advancements seen in radical *S*-glycosylation methodologies. Furthermore, diverse bioactive compounds and pharmaceuticals were successfully glycosylated. This highlights the method's functional group tolerance and its potential utility for enhancing crucial drug properties, such as aqueous solubility. The ability to readily introduce 2-deoxyglycan motifs onto these intricate structures underscores the practical value of this photo-promoted approach for late-stage molecular functionalization.

Following the successful application of carboxylic acids, we investigated the scope of alcohol nucleophiles (Fig. 4). A diverse array of primary and secondary aliphatic alcohols served as competent glycosyl acceptors, readily participating in the reaction to afford the corresponding α–2-deoxyglycosides (**6a**–**6m**) in moderate to good yields, typically with moderate α-stereoselectivity. The mild, metal-free nature of the reaction ensured broad functional group compatibility, tolerating various sensitive moieties. Consistent with steric control, competition experiments demonstrated chemoselectivity, favoring reaction with primary alcohols over more hindered tertiary alcohols (*e.g.*, formation of **6e**). Importantly, the protocol's utility extended to structurally complex and functionally diverse alcohols. *N*-Boc protected amino alcohols, chiral secondary alcohols, and carbohydrate derivatives all reacted smoothly, yielding the desired glycosylated products (**6n**–**6x**) and showcasing the method's robustness. This broad applicability to different alcohol classes further establishes this photo-promoted strategy as a valuable tool for accessing diverse α–2-deoxyglycosides under mild conditions.

To elucidate the reaction pathway underlying this photo-induced 2-deoxyglycosylation, a series of mechanistic experiments were conducted (Fig. 5). Control reactions confirmed that both the acridinium salt (**PC1**) and visible light irradiation are essential for product formation (Table 1), consistent with a photo-initiated process. When the model reaction between glycal **1a** and benzoic acid **2a** was performed in the presence of 2 equiv. of the radical scavenger TEMPO, glycosylation was significantly suppressed (<2% yield), implicating the involvement of radical intermediates

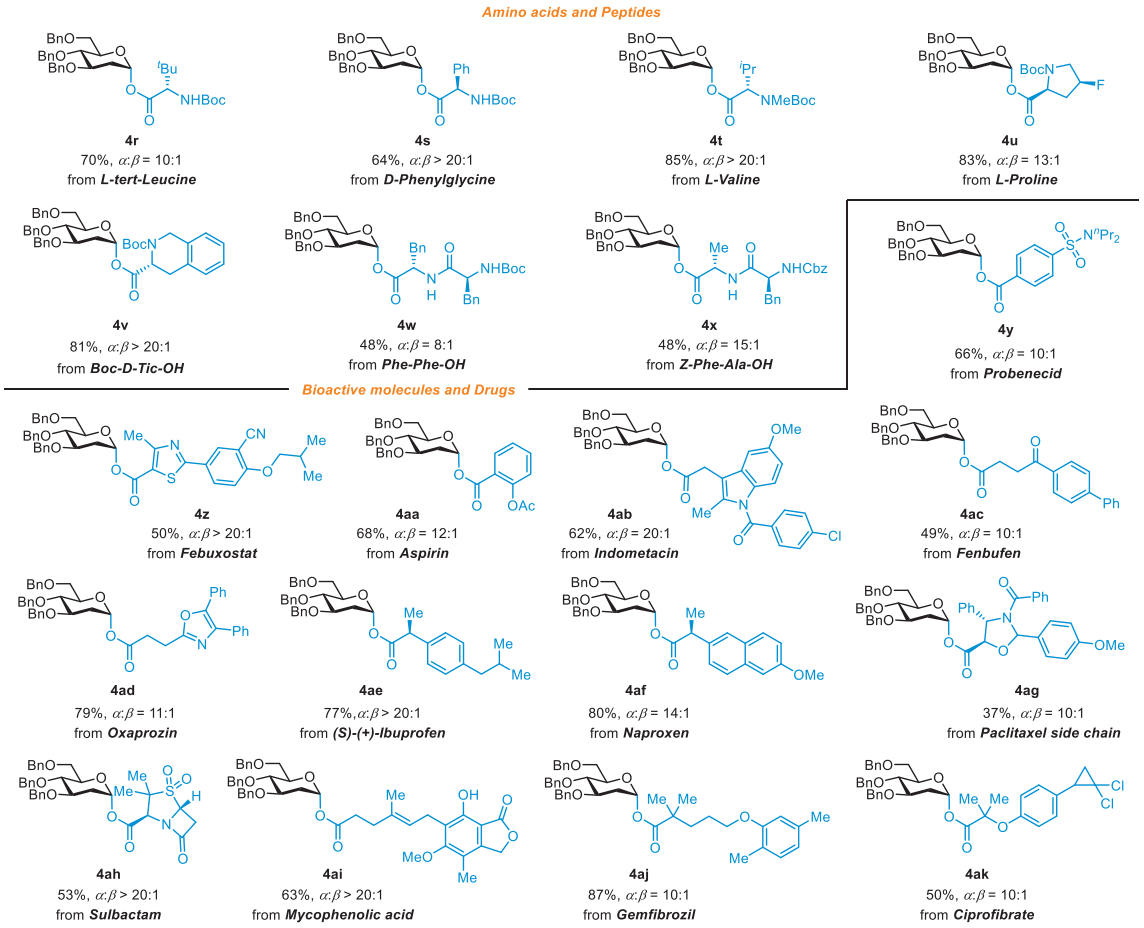


Fig. 3. The scope of 2-deoxyglycosylation for natural products and bioactive compounds.

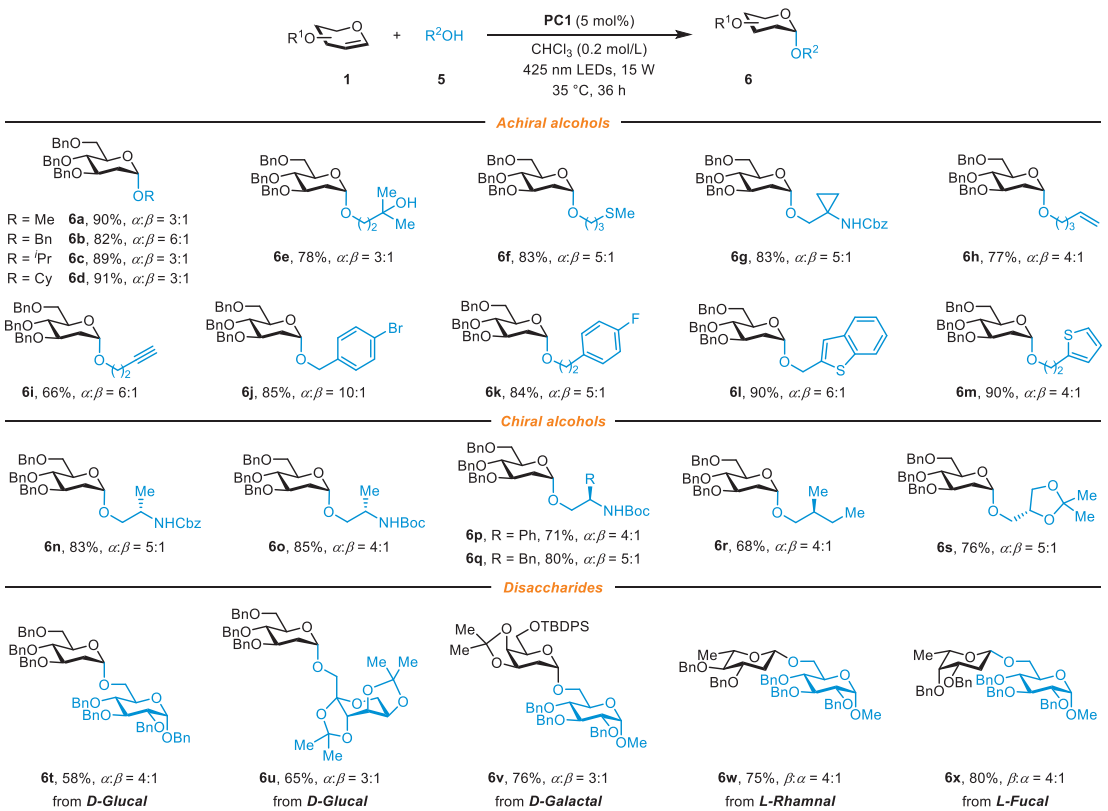


Fig. 4. The scope of alcohols for the stereoselective *O*-glycosylation of glycals.

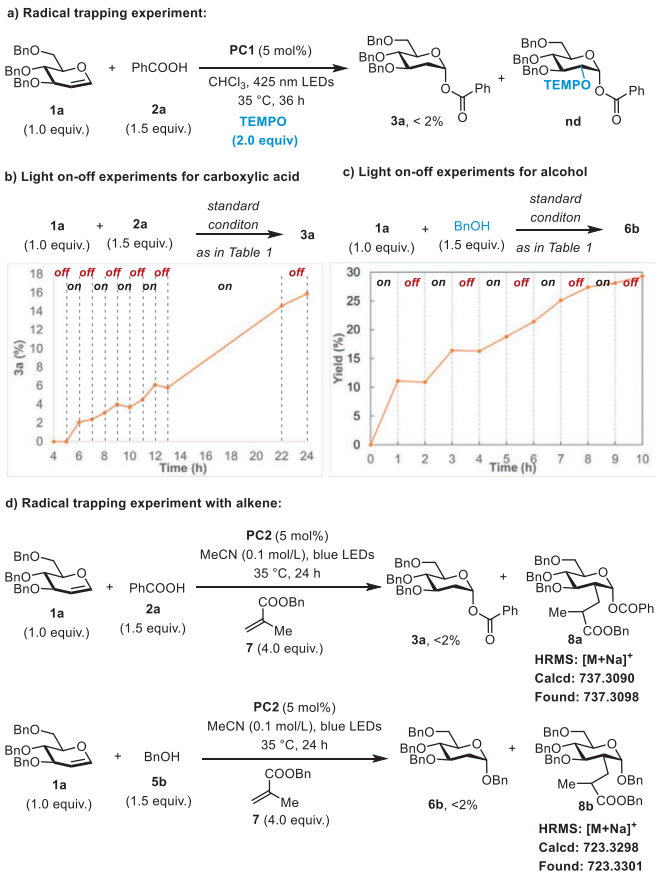
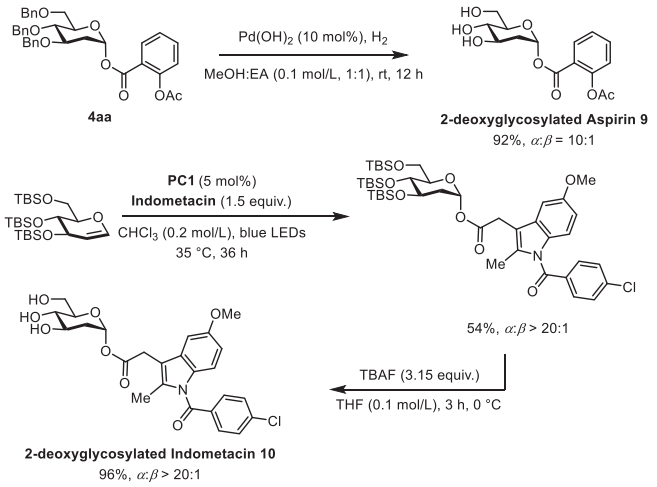


Fig. 5. Mechanistic investigations.



Scheme 1. Synthesis of 2-deoxyglycosylated aspirin and indomethacin.

(Fig. 5a). However, no TEMPO adducts were definitively detected via mass spectrometry, preventing unambiguous confirmation of direct radical trapping under these specific conditions. Light on-off experiments provided further insight; the reaction employing benzoic acid exhibited a distinct induction period and, crucially, continued to proceed after the light source was removed (Fig. 5b). This observation suggests the operation of a chain-reaction mechanism, or the formation of a persistent active catalytic species generated under irradiation. A similar light on-off experiment using benzyl alcohol nucleophile also showed continued reaction progress in the dark, although without a noticeable induction period (Fig. 5c). To probe specific radical intermediates, a trapping experiment was designed using unsaturated alkene **7**, known to intercept alkyl radicals. Under slightly modified conditions, these experiments yielded no expected glycosylation product **3a** or **6b** but resulted in HRMS evidence for the formation of possible adducts **8a** and **8b**, potentially arising from the trapping of a C-2 centered alkyl radical derived from the glycal (Fig. 5d). Collectively, these preliminary results suggest a complex mechanism. While distinct from photo-promoted pathways reported to cease upon light removal, the current data accommodate several possibilities, including nucleophilic addition to a photogenerated glycal radical cation, a radical chain process, or the generation of an alternative catalytically active species [35,39,40,47]. Further detailed kinetic and spectroscopic studies are required to distinguish between these potential pathways.

Having elucidated the potential photo-promoted pathway underlying this methodology, we next sought to evaluate its functional utility by applying the protocol to the 2-deoxyglycosylation of NSAIDs, probing the impact of glycosylation on their biological activity. With our protocol, the 2-deoxyglycosylated aspirin **9** and indomethacin **10** were successfully synthesized (Scheme 1). Previous studies have suggested the neuroprotective effects of NSAIDs at the cellular level [48,49]. We thus examined the neuronal growth after treatment with aspirin or modified-aspirin, as the classic and most commonly used type of NSAID. Indeed, both these chemicals at an optimal dose of 100 μmol/L favored neuronal growth in primary hippocampal neuron culture at 11 days *in vitro* (DIV) (Figs. 6a and b). Furthermore, modified-aspirin exhibited a more potent effect in promoting neuronal dendrite growth compared with aspirin, demonstrated by a significant increase in dendritic intersections and area under the curve (AUC) in Sholl analysis (Figs. 6c-f) [50]. Similarly, modified-indomethacin also promoted neuronal growth and significantly enhanced dendritic complexity and arborization compared with indomethacin, at a recommended dosage (Figs. 6g-l) [51]. These data collectively indicated that the addition of sugar-epitopes to aspirin and indomethacin significantly strengthen their neuroprotective potency and promotes neuronal development at the early stage. Dendritic complexity, reflected by the branching, length, and interconnections, determines neuronal connectivity and communication through expanding synaptic surface area, allowing neurons to integrate inputs and sustain higher-order functions like learning, memory, and plasticity [52,53]. Deficits in dendritic structure are hallmark features of numerous neurodevelopmental and neurodegenerative disorders, including autism spectrum disorder, Fragile X syndrome, schizophrenia and Alzheimer's disease, where disrupted connectivity correlates with cognitive and behavioral impairments [53,54]. By identifying a chemical strategy that potently enhance the capability of compound for promoting dendritic growth, our work suggests a potential therapeutic strategy to ameliorate structural deficits in brain disorders, though future studies must validate efficacy *in vivo* and assess risks of unintended circuit formation to balance enhanced connectivity with neurological safety.

We next examined whether structural plasticity induced by modified NSAIDs extends beyond accelerating dendritic maturation to functionally enhance synapse development critical for circuit integrity. To evaluate this, we quantified the density and size of PSD-95, a postsynapse-enriched scaffolding protein essential for synaptic stability, maturation, and activity-dependent plasticity [55,56]. Both modified-aspirin and modified-indomethacin significantly increased the density and size of PSD-95 puncta compared with aspirin or indomethacin, indicative of a more mature stage of synapse (Figs. 7a-f). Kainic acid (KA) is a nondegradable structural analog to glutamate and therefore acts as a neurotoxic chemical, leading to an increase of inflammatory molecules followed by neu-

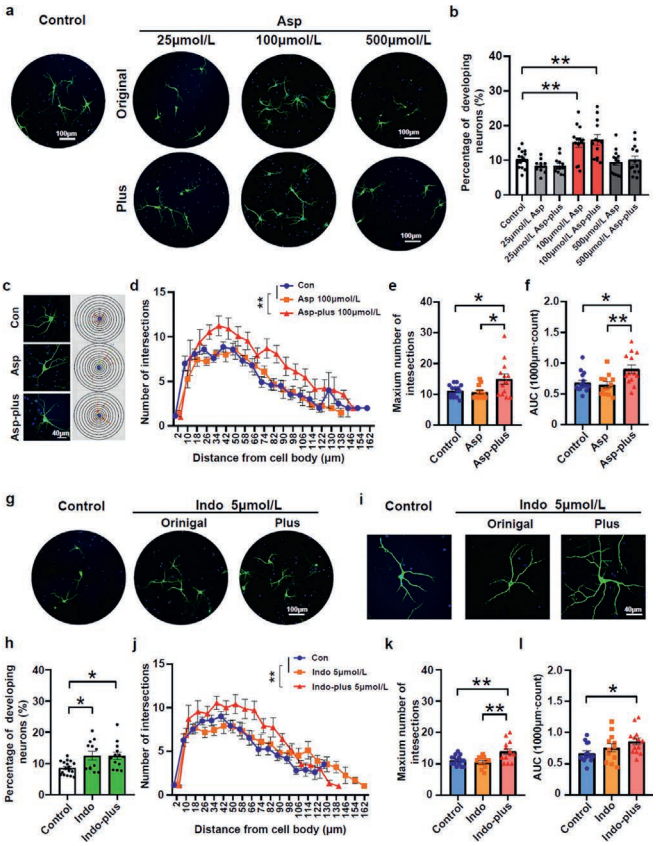


Fig. 6. Sugar-modified aspirin or indomethacin favors neuronal growth and promotes dendrite development. (a) Representative images of primary cultured hippocampal neurons treated with compounds as indicated. Scale bar: 100 μm. (b) Quantification of the percentage of developing neurons. n = 15, 12, 12, 13, 13, 14, 13 regions for control, aspirin (Asp) and 2-deoxyglycosylated aspirin (Asp-plus) at 25, 100 and 500 μmol/L, respectively. (c) Representative images of single hippocampal neuron treated with compounds as indicate (left), and images processed by Sholl analysis (right). Scale bar: 40 μm. (d) The dendritic complexity of hippocampal neurons analyzed by Sholl analysis. (e) Quantification of maximum intersection numbers in (d). (f) Quantification of the area under curve (AUC) shown in (d). For (d-f), n = 15, 12 and 13 neurons for control, Asp and Asp-plus groups. (g) Representative images of primary cultured hippocampal neurons treated with compounds as indicated. Scale bar: 100 μm. (h) Quantification of the percentage of developing neurons. n = 18, 12, 13 regions for Control, Indomethacin (Indo) and 2-deoxyglycosylated Indo (Indo-plus) conditions, respectively. (i) Representative images of single hippocampal neuron treated with compounds as indicated. Scale bar: 40 μm. (j) The dendritic complexity of hippocampal neurons analyzed by Sholl analysis. (k) Quantification of maximum intersection numbers in (j). (l) Quantification of the AUC shown in (j). For (j-l), n = 15, 12 and 13 neurons for control, Indo and Indo-plus groups, respectively. For all images, neurons at 11 DIV were co-stained with MAP-2 (green) and DAPI (blue). All data are shown as the mean ± SEM. $^{*}P < 0.05$, $^{**}P < 0.01$.

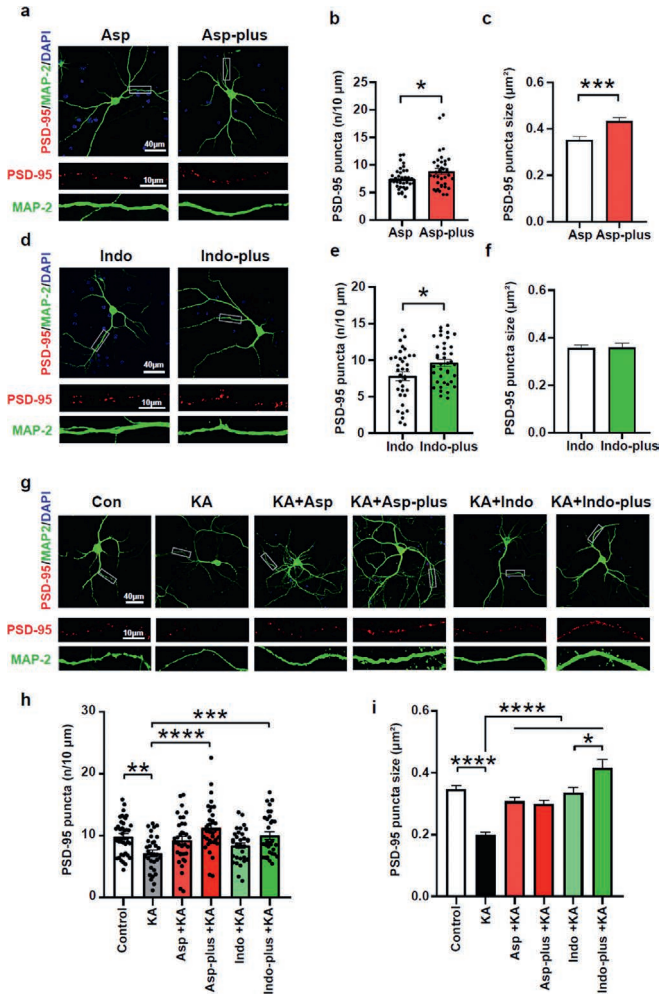


Fig. 7. Sugar-modified aspirin or indomethacin promotes synapse maturation and protects neuron from KA-induced neurotoxicity. (a) Representative images of primary cultured hippocampal neurons (upper) and cropped dendrites (lower). (b) Quantification of PSD-95 puncta density. (c) Quantification of PSD-95 puncta size. For (b, c), n = 35 and 36 dendrites from 12 neurons each for Asp and Asp-plus groups. (d) Representative images of primary cultured hippocampal neurons (upper) and cropped dendrites (lower). (e) Quantification of PSD-95 puncta density. (f) Quantification of PSD-95 puncta size. For (e, f), n = 35 and 39 dendrites from 12 and 13 neurons for Indo and Indo-plus groups, respectively. (g) Representative images of primary cultured hippocampal neurons (upper) and cropped dendrites (lower). (h) Quantification of PSD-95 puncta density. (i) Quantification of PSD-95 puncta size. For (h, i), n = 38, 32, 34, 34, 33 and 32 dendrites from 14, 11, 12, 12, 11 and 11 neurons for control, KA, KA with Asp or Asp-plus, KA with Indo or Indo-plus treatment groups, respectively. For all images, neurons treated with indicated chemicals were fixed at 17 DIV and co-stained with PSD-95 (red) and MAP-2 (green). Scale bar: 40 μm (for neuron) and 10 μm (for dendrite). All data are shown as the mean ± SEM. $^{*}P < 0.05$, $^{**}P < 0.01$, $^{***}P < 0.001$, $^{****}P < 0.0001$.

ronal death [57,58]. KA treatment has been found to cause pathological changes in rodent brains and is commonly used to mimic the human neurodegenerative disorders [59,60]. Indeed, both density and size of the PSD-95 puncta got significantly reduced after KA treatment in cultured hippocampal neurons. Notably, either modified-aspirin or modified-indomethacin rather than their original forms restored the state of PSD-95 to as comparable as the control group (Figs. 7g-i). By integrating *O*-glycosylation's capacity to enhance dendritic complexity with its ability to stabilize synapses against KA-induced excitotoxicity, our strategy uniquely addresses both the structural and functional deficits underlying neurodevelopmental and neurodegenerative disorders, offering a unified intervention to mitigate cognitive deficits rooted in synaptic dysfunctions.

In summary, we have developed an efficient, metal-free *O*-glycosylation methodology for the synthesis of 2-deoxyglycosides from readily available glycals using acridinium salts under visible light irradiation. This protocol successfully accommodates both carboxylic acids and a wide range of alcohols, including complex and functionally diverse examples, as nucleophiles. Key features of this transformation include its operational simplicity, mild reaction conditions, broad substrate scope, excellent functional group tolerance, and notable α-stereoselectivity, particularly with carboxylic acid acceptors. The applicability to late-stage functionalization of bioactive molecules, amino acids, and peptides highlights its potential utility in drug discovery and glycoconjugate chemistry. Preliminary mechanistic investigations point towards a photo-initiated radical pathway, possibly involving a chain mech-

anism, offering a distinct reactivity profile compared to traditional glycosylation methods. Moreover, the biological evaluation of 2-deoxyglycosylated NSAIDs prepared using this method demonstrated significantly enhanced neurotrophic and neuroprotective effects *in vitro*, suggesting that such modifications can potentiate therapeutic activity. This study establishes photo-induced glycosylation as a valuable addition to the synthetic toolkit for accessing challenging 2-deoxyglycan structures and provides a foundation for further exploration of photoredox reactions in carbohydrate chemistry and its application in developing novel therapeutics. Future work will focus on deeper mechanistic elucidation and expanding the application scope, including *in vivo* validation of the observed biological effects.

Declaration of competing interest

The authors declare that they have no known competing financial interests or personal relationships that could have appeared to influence the work reported in this paper.

CRediT authorship contribution statement

Xianrong Zeng: Writing – review & editing, Writing – original draft, Project administration, Methodology, Investigation, Formal analysis, Data curation. **Hui-Ying Shi:** Writing – original draft, Project administration, Methodology, Formal analysis, Data curation. **Huiqian Huang:** Writing – review & editing, Writing – original draft, Supervision, Project administration, Investigation, Formal analysis, Data curation, Conceptualization. **Zhaobin Wang:** Writing – review & editing, Writing – original draft, Supervision, Project administration, Investigation, Conceptualization.

Acknowledgments

We are grateful for financial support from the National Natural Science Foundation of China (No. 22171231), Zhejiang Provincial Key Laboratory Construction Project, Zhejiang Provincial Natural Science Foundation of China (No. XHD23B0101), and National Natural Science Foundation of China (No. 82471531). We thank Westlake University Instrumentation and Service Center for Molecular Science and Physical Sciences for the assistance in measurement and data interpretation. We thank the Core Facilities of the Zhejiang University Institute of Neuroscience for technical assistance.

Supplementary materials

Supplementary material associated with this article can be found, in the online version, at doi:10.1016/j.cclet.2025.111615.

References

[1] G.W. Yip, M. Smollich, M. Gotte, Mol. Cancer Ther. 5 (2006) 2139–2148.
[2] I. Popa, A. Pons, C. Mariller, et al., Glycobiology 17 (2007) 367–373.
[3] K.S. Lau, J.W. Dennis, Glycobiology 18 (2008) 750–760.
[4] S.M. Muthana, C.T. Campbell, J.C. Gildersleeve, ACS Chem. Biol. 7 (2012) 31–43.
[5] M. Suflita, L. Fu, W. He, M. Koffas, R.J. Linhardt, Appl. Microbiol. Biotechnol. 99 (2015) 7465–7479.
[6] J. Munkley, I.G. Mills, D.J. Elliott, Nat. Rev. Urol. 13 (2016) 324–333.
[7] M.M. Wei, Y.S. Wang, X.S. Ye, Med. Res. Rev. 38 (2018) 1003–1026.
[8] P.H. Seeberger, D.B. Werz, Nature 446 (2007) 1046–1051.
[9] C. Reily, T.J. Stewart, M.B. Renfrow, J. Novak, Nat. Rev. Nephrol. 15 (2019) 346–366.
[10] Y.S. Wijayasinghe, M.P. Bhansali, M.R. Borkar, et al., J. Med. Chem. 65 (2022) 3706–3728.
[11] I. Prassas, E.P. Diamandis, Nat. Rev. Drug Discov. 7 (2008) 926–935.
[12] J.-T. Zheng, U. Rix, L. Zhao, et al., J. Antibiot. 58 (2005) 405–408.
[13] R.T. Crow, B. Rosenbaum, R. Smith, et al., Bioorg. Med. Chem. Lett. 9 (1999) 1663–1666.
[14] C.S. Bennett, M.C. Galan, Chem. Rev. 118 (2018) 7931–7985.
[15] Y. Yang, B. Yu, Chem. Rev. 117 (2017) 12281–12356.
[16] P. Peng, R.R. Schmidt, Acc. Chem. Res. 50 (2017) 1171–1183.
[17] M.J. McKay, H.M. Nguyen, ACS Catal. 2 (2012) 1563–1595.
[18] C.J. Crawford, P.H. Seeberger, Chem. Soc. Rev. 52 (2023) 7773–7801.
[19] K. Yamatsugu, M. Kanai, Chem. Rev. 123 (2023) 6793–6838.
[20] J. Zeng, Y. Xu, H. Wang, L. Meng, Q. Wan, Sci. China Chem. 60 (2017) 1162–1179.
[21] C.K. Prier, D.A. Rankic, D.W.C. MacMillan, Chem. Rev. 113 (2013) 5322–5363.
[22] N.A. Romero, D.A. Nicewicz, Chem. Rev. 116 (2016) 10075–10166.
[23] L. Marzo, S.K. Pagire, O. Reiser, B. König, Angew. Chem. Int. Ed. 57 (2018) 10034–10072.
[24] G.E.M. Crisenza, P. Melchiorre, Nat. Commun. 11 (2020) 803–806.
[25] W.F. Zhu, C. Empel, S. Pelliccia, et al., J. Med. Chem. 67 (2024) 4322–4345.
[26] C.E. Suh, H.M. Carder, A.E. Wendlandt, ACS Chem. Biol. 16 (2021) 1814–1828.
[27] W. Shang, D. Niu, Acc. Chem. Res. 56 (2023) 2473–2488.
[28] C. Zhang, H. Zuo, G.Y. Lee, et al., Nat. Chem. 14 (2022) 686–694.
[29] L.F. Deng, Y. Wang, S. Xu, et al., Science 382 (2023) 928–935.
[30] H. Zuo, C. Zhang, Y. Zhang, D. Niu, Angew. Chem. Int. Ed. 62 (2023) e202309887.
[31] G. Zhao, W. Yao, I. Kevlishvili, et al., J. Am. Chem. Soc. 143 (2021) 8590–8596.
[32] G. Zhao, W. Yao, J.N. Mauro, M.Y. Ngai, J. Am. Chem. Soc. 143 (2021) 1728–1734.
[33] W. Yao, G. Zhao, Y. Wu, et al., J. Am. Chem. Soc. 144 (2022) 3353–3359.
[34] G. Zhao, U. Mukherjee, L. Zhou, et al., CCS Chem. 5 (2023) 106–116.
[35] F. Wu, L. Wang, Y. Ji, J. Chen, Y. Huang, et al., iScience 23 (2020) 101395.
[36] D.S. Hamilton, D.A. Nicewicz, J. Am. Chem. Soc. 134 (2012) 18577–18580.
[37] N.A. Romero, D.A. Nicewicz, J. Am. Chem. Soc. 136 (2014) 17024–17035.
[38] D.J. Wilger, J.M.M. Grandjean, T.R. Lammert, D.A. Nicewicz, Nat. Chem. 6 (2014) 720–726.
[39] G. Zhao, T. Wang, Angew. Chem. Int. Ed. 57 (2018) 6120–6124.
[40] K.M. Liu, P.Y. Wang, Z.Y. Guo, et al., Angew. Chem. Int. Ed. 61 (2022) e202114726.
[41] D. Crich, F. Cai, Org. Lett. 9 (2007) 1613–1615.
[42] Y. Yang, Y. Li, B. Yu, Tetrahedron Lett. 51 (2010) 1504–1507.
[43] H.Y. Wang, C.J. Simmons, Y. Zhang, et al., Org. Lett. 19 (2017) 508–511.
[44] T. Yang, F. Zhu, M.A. Walczak, Nat. Commun. 9 (2018) 3650–3658.
[45] Z. Liu, D. Liu, D. Zhu, B. Yu, Org. Lett. 25 (2023) 5372–5377.
[46] S. Fukuzumi, H. Kotani, K. Ohkubo, et al., J. Am. Chem. Soc. 126 (2004) 1600–1601.
[47] S. Das, D. Pekel, J.-M. Neudörfl, A. Berkessel, Angew. Chem. Int. Ed. 54 (2015) 12479–12483.
[48] E. Auriel, K. Regev, A.D. Korczyn, Handb. Clin. Neurol. 119 (2014) 577–584.
[49] E.G. Hain, M. Sparenberg, J. Rasińska, et al., J. Neuroinflammation 15 (2018) 162.
[50] D.A. Sholl, J. Anat. 87 (1953) 387–406.
[51] W. Sun, M. Wang, J. Zhao, et al., Nat. Commun. 14 (2023) 5351–5367.
[52] A.A. Galakhova, S. Hunt, R. Wilbers, et al., Trends Cogn. Sci. 26 (2022) 909–922.
[53] V.A. Kulkarni, B.L. Firestein, Mol. Cell. Neurosci. 50 (2012) 10–20.
[54] M.P. Forrest, E. Parnell, P. Penzes, Nat. Rev. Neurosci. 19 (2018) 215–234.
[55] A.E. El-Husseini, E. Schnell, D.M. Chetkovich, R.A. Nicoll, D.S. Bredt, Science 290 (2000) 1364–1368.
[56] I. Ehrlich, M. Klein, S. Rumpel, R. Malinow, Proc. Natl. Acad. Sci. U. S. A. 104 (2007) 4176–4181.
[57] G.M. Kasof, A. Mandelzys, S.D. Maika, et al., J. Neurosci. 15 (1995) 4238–4249.
[58] J. Garthwaite, G. Garthwaite, Nature 305 (1983) 138–140.
[59] J. Talbot, S. Chear, A. Phipps, et al., Methods Mol. Biol. 2549 (2022) 187–207.
[60] Q. Wang, S. Yu, A. Simonyi, G.Y. Sun, A.Y. Sun, Mol. Neurobiol. 31 (2005) 3–16.